Forcing of the Summertime Low-Level Jet along the California Coast

THOMAS R. PARISH

Department of Atmospheric Science, University of Wyoming, Laramie, Wyoming

(Manuscript received 29 October 1999, in final form 7 April 2000)

ABSTRACT

Coast-parallel low-level jets are commonplace in the offshore environment along the west coast of the United States during summer. The jet often has wind speeds in excess of 30 m s^{-1} and is typically situated near the top of the marine boundary layer. A field study was conducted in early summer of 1997 to study the kinematics and dynamics of the low-level jet off the California coast. The University of Wyoming King Air research aircraft was the primary observation platform. Measurement of the horizontal pressure gradient force was fundamental to understanding the dynamics of the jet. By flying at constant pressure, the height of an isobaric surface could be determined by the radar altimeter. The slope of a constant pressure surface is proportional to the pressure gradient force and hence provides an estimate of the geostrophic wind.

Data are presented for two episodes of the low-level jet. In both cases wind speed maxima extending in excess of 100 km from the coast were observed. In contrast to previous observational studies, little evidence of hydraulic effects near the coastal margin was found. Measurements of the horizontal pressure gradient force within the marine boundary layer showed that the coastal jet is in a state of near-geostrophic balance. The observed vertical shear of the geostrophic wind components matched direct measurements of the thermal wind and confirms the importance of the sloping marine boundary layer in forcing the jet as proposed previously. It is offered that the large-scale structure of sloping marine layer and its attendant low-level jet is consistent with the geostrophic adjustment of thermally direct circulation forced by the horizontal temperature contrast between land and ocean.

1. Introduction

The term ''low-level jet'' (LLJ) is commonly used in meteorological literature to describe a wide variety of wind features found over nearly every continent on earth (see Bonner 1968; Uccellini and Johnson 1979; Li and Chen 1998; and references contained therein). Some authors have used the term to describe any low-level wind maximum while others (e.g., Bonner 1968) take care to define appropriate wind shear criteria and threshold values of the wind maximum before applying the term low-level jet. Because of the widespread LLJ occurrence and diversity of physical characteristics, the term low-level jet is subject to wide interpretation. In addition, the various LLJ features represent a diverse set of forcing conditions.

Perhaps the best known jet is the Great Plains LLJ (Blackadar 1957; Hoecker 1963; Bonner 1968; McNider and Pielke 1981; Parish et al. 1988; Arritt et al. 1997; Whiteman et al. 1997). Observations show that this jet is present over a wide geographic region from the sloping plains east of the Rocky Mountains to the Mississippi River. This class of LLJ is highly ageostrophic, with maximum wind speeds reached shortly after midnight. Observational studies (Kaimal and Izumi 1965; Parish et al. 1988) suggest that this LLJ occurs primarily as a result of inertial oscillations resulting from the sudden decrease in the friction force during evening (Blackadar 1957). The role of diabatic heating and cooling of the sloping terrain has also been linked to the evolution of the Great Plains LLJ (Holton 1967).

A second example of a LLJ is the so-called barrier jet (e.g., Schwerdtfeger 1979; Parish 1982, 1983; Li and Chen 1998). This jet is a mountain-parallel wind maximum resulting from the geostrophic adjustment as stable air is advected against an elongated topographic ridge. This class of LLJ is near-geostrophic in a direction parallel to the barrier but has significant ageostrophic components perpendicular to the ridge. It has characteristics similar to a class of LLJs produced by cold-air blocking or damming (e.g., Bell and Bosart 1988). A third class of LLJ occurs as a result of the secondary circulation associated with an upper-tropospheric jet core as suggested by Uccellini and Johnson (1979) and Brill et al. (1985). Significant ageostrophic components are present as part of the mass adjustments associated with this LLJ. In particular, the isallobaric wind in the lower atmosphere perpendicular to the upper jet axis was shown to be dominant.

Corresponding author address: Thomas R. Parish, Department of Atmospheric Science, University of Wyoming, Room 6034, Engineering Building, Box 3038, Laramie, WY 82071.
E-mail: parish@uwyo.edu

A fourth example is the LLJ feature found along coastal regions (Zemba and Friehe 1987; Doyle and Warner 1991; Douglas 1995; Burk and Thompson 1996; Holt 1996). Thermal wind processes associated with land–sea heating contrasts have been identified as fundamental to the structure of these LLJs. Topography also can play a role in providing local enhancements near the coastal zone. Observations (e.g., Beardsley et al. 1987) have shown that the series of coastal points and capes along the California coast lead to significant acceleration of the flows in the lower atmosphere. Winant et al. (1988), Samelson (1992), and Burk and Thompson (1996), among others, discuss the local terrain influences on the jet.

This brief discussion is not intended to be comprehensive, but rather to point out the diversity of wind maxima that have been classified under the term low-level jet. From a dynamical perspective, each of the aforementioned classes of LLJ differs considerably from one another. The purpose of this paper is to report on direct measurements of the dynamics responsible for the fourth class of LLJ along the California coast during June 1997, and to compare with previous observations and analyses. For the purposes of this discussion, such a LLJ will be denoted as a ''coastal jet'' (CJ). A discussion of the CJ and results of previous studies are presented in section 2. Section 3 describes the two case study days and airborne observations of the CJ, and contrasts the observations with previous findings. Airborne measurements of the horizontal pressure gradient force associated with the CJ are discussed in section 4. Direct measurements of the thermal wind in the marine boundary layer are given in section 5 and a summary is provided in section 6.

2. The summertime coastal jet off the California coast

During summer the wind and pressure fields off the coasts of California and Oregon are influenced significantly by the broad Pacific high, situated about 1000 km to the west. Winds in the boundary layer off the west coast of the United States are predominantly from a north or northwesterly direction, roughly parallel to the orientation of the coastline. Frequently, the low-level wind field is characterized by a sharp wind maximum at a height of approximately 300–400 m, and a distinct jet profile. Peak winds associated with the CJ in excess of 30 m s^{-1} have been observed (e.g., Zemba and Friehe 1987; Beardsley et al. 1987). The jet is tied to the thermal structure of the marine planetary boundary layer (MBL). Neiburger et al. (1961) notes that strong subsidence exists along the eastern flank of the Pacific high, producing a marked temperature inversion at the top of the well-mixed MBL. Previous studies have shown that the core of the LLJ is found at the top of the MBL (Burk and Thompson 1996; Rogers et al. 1998). The height of the inversion has been shown to increase to the west (Neiburger et al. 1961) and thus the height of the wind maximum displays a gradual increase in a westward direction.

There have been several observational studies of the MBL and associated CJ. Zemba and Friehe (1987) have examined the vertical and horizontal boundary layer structure off the west coast of the United States as part of the Coastal Ocean Dynamics Experiment (CODE). Results of the study indicated that the thermal wind resulting from the strong horizontal temperature contrast between land and ocean is fundamentally responsible for the jet profile. Beardsley et al. (1987) have also examined the coastal jet during CODE, and emphasize the effects of diurnal heating on the observed near-coastal winds. Gerber et al. (1989) used tethered balloons to document the boundary layer off the West Coast and also noted the importance of the thermal wind in forcing of a coastal jet. Samelson and Lentz (1994), using meteorological data collected from an array of surface buoys during CODE, analyzed the momentum balance of the MBL. Their results suggest that significant orographic modifications of the boundary layer occur in the vicinity of the coast. Other related studies of the MBL with reference to the low-level wind field include Elliot and O'Brien (1977), Brost et al. (1982), Lester (1985), and Bridger et al. (1993). More recently, Rogers et al. (1998) have conducted a series of flights to explore the boundary layer off the West Coast. Their flights included several that specifically focused on the low-level wind structure near the northern California coast. Results show a strong CJ with maxima that appear to be tied to the local terrain. The CJ has maximum winds of 25 m s^{-1} approximately 20 km offshore (Roger et al. 1998). Coastal wind phenomena have also attracted the attention of modelers, including Chao (1985), Winant et al. (1988), Gerber et al. (1989), Samelson (1992), Holt (1996), Burk and Thompson (1996), and Burk et al. (1999).

A field study focusing on the airflow in the MBL off the California coast was conducted during June 1997. The University of Wyoming King Air (K/A) research aircraft was the primary observation platform. Examination was made into the kinematic structure and dynamics responsible for the CJ off the central and northern California coast during June 1997. Seven dedicated LLJ missions were conducted during the field study period. Table 1 provides details as to the flight objectives, strength, and position of the CJ.

Emphasis was also placed on documenting episodes of southerly wind reversals known as coastally trapped disturbances (CTDs). Approximately twice each month during summer, the low-level northerly flow pattern off the West Coast is replaced by a propagating southerly wind regime in a narrow zone on the order of 100 km adjacent to the coastline (Bond et al. 1996). These CTDs are accompanied by fog, rising pressure, and a cooling of approximately 10 K and propagate northward along the coast at speeds up to 5 m s^{-1} (e.g., Dorman 1985;

TABLE 1. Summary of low-level jet K/A flights during June 1997.

Date	Location	Objective	Jet speed	Comments
6 Jun	Half Moon Bay	Intercomparison, LLJ	30 m s^{-1}	Uniform jet 50–100 km offshore
7 Jun	Half Moon Bay	LLJ forcing	28 m s^{-1}	Maximum jet 100 km offshore
8 Jun	Cape Mendocino–Monterey Bay	Topographic forcing	25 m s^{-1}	Little evidence of coastal hydraulic effects
13 Jun	Half Moon Bay	LLJ forcing	28 m s^{-1}	Well-defined LLJ, strongest jet situated $>$ 150 km from coast
15 Jun	South of Monterey Bay	Mini-CTD?	none	Nonpropagating, southerly flow
20 Jun (1600 UTC)	Half Moon Bay	Diurnal variation LLJ	25 m s^{-1}	Uniform jet 50–100 km offshore
21 Jun (0100 UTC)	Half Moon Bay	Diurnal variation LLJ	25 m s^{-1}	Weak diurnal variation

Nuss 1995; Bond et al. 1996; Ralph et al. 1998 and references contained therein). No wind reversals were observed during the June 1997 study.

3. Structure of the coastal LLJ during June 1997

A large anticyclone was situated to the west of the northern California coast for much of the month and dominated the low-level flow conditions across the eastern Pacific and the west coast of the United States. Examples of the large-scale synoptic situation on case study days are shown in Fig. 1. The fields of sea level pressure at 0000 UTC 8 June and 1800 UTC 13 June 1997 are based on the National Centers for Environmental Prediction (NCEP) Eta Model analysis. Both cases show that a northerly low-level wind field was present over a broad area of the eastern Pacific adjacent to the West Coast from Washington to California. The strongest horizontal pressure gradient force (PGF) on both days is seen off the northern California coast. The target area for the June 1997 research flights was west of Half Moon Bay, south of the San Francisco area. The flight strategies (Fig. 2) consisted of a series of sawtooth flight maneuvers between 50 and 1500 m altitude along approximately 37.5°N to sample the cross flow structure. Additional sawtooth profiles were conducted in a north–south direction along 123.2°W on 7 June, and in the east–west direction to the west of Monterey Bay along 36.8°N also on 7 June. The sawtooth legs were between 100 and 150 km in length in order to sample the wind field at extended distances from the central California coast. Each flight also incorporated a series of 50–70 km isobaric legs at levels near the jet maximum. The purpose of these legs was to measure the slope of a constant pressure surface near the level of the CJ maximum and hence determine the PGF. Orthogonal isobaric legs were flown to enable measurements of the PGF in directions perpendicular and parallel to the flow as well. Clear skies prevailed throughout both flights.

It has been noted (Neiburger et al. 1961) that the summertime marine inversion has a mean height of about 400 m just off the California coast, rising toward the west adjacent to the coast. Subsequent studies (i.e., Brost et al. 1982; Beardsley et al. 1987; Zemba and Friehe 1987) have confirmed the general inversion height progression and provide valuable observations of the wind field in the MBL. This sloping inversion height is fundamental to the CJ development (Zemba and Friehe 1987) and was observed on each of the seven case study flights. Figure 3 shows the total wind speed and potential temperature profiles for the 7 and 13 June 1997 flights obtained from the east–west sawtooth maneuvers. The soundings were obtained from the K/A platform during the 7 June ascents and 13 June descents (see Fig. 2 for positions). The wind profiles each show a well-defined jet near the top of the MBL. Wind speeds display a monotonic westward increase in both CJ intensity and the jet height. Maximum wind speeds at a distance of 30 km from the coast were approximately 15 and 19 m s^{-1} on 7 and 13 June, respectively, increasing to nearly 30 m s^{-1} at the westernmost sounding. Note that the maximum observed wind speeds associated with the CJ are seen over 175 km from the coast on 13 June, and it is possible that higher CJ winds are found to the west of the last sounding on each day. Wind speeds decreased abruptly below the jet core, presumably due to the turbulent transfer of momentum to the surface. A strong decrease in wind speed is also seen above the inversion in response to the pronounced decrease in the horizontal pressure gradient owing to the thermal wind associated with the sloping MBL (Zemba and Friehe 1987). Wind directions in the lower marine atmosphere (not shown) displayed less pronounced vertical and horizontal changes. In general, wind directions in the MBL in each case veered by 20° to 30° between 100 m above the ocean to top of the MBL. In all probability, this directional shear occurs in response to the decrease in the friction force with height. Wind directions above the inversion remain primarily from the north and display little change to 2000 m.

The thermal structure of the lower atmosphere for each day reveals a well-mixed MBL capped by warmer air associated with subsidence from the Pacific high.

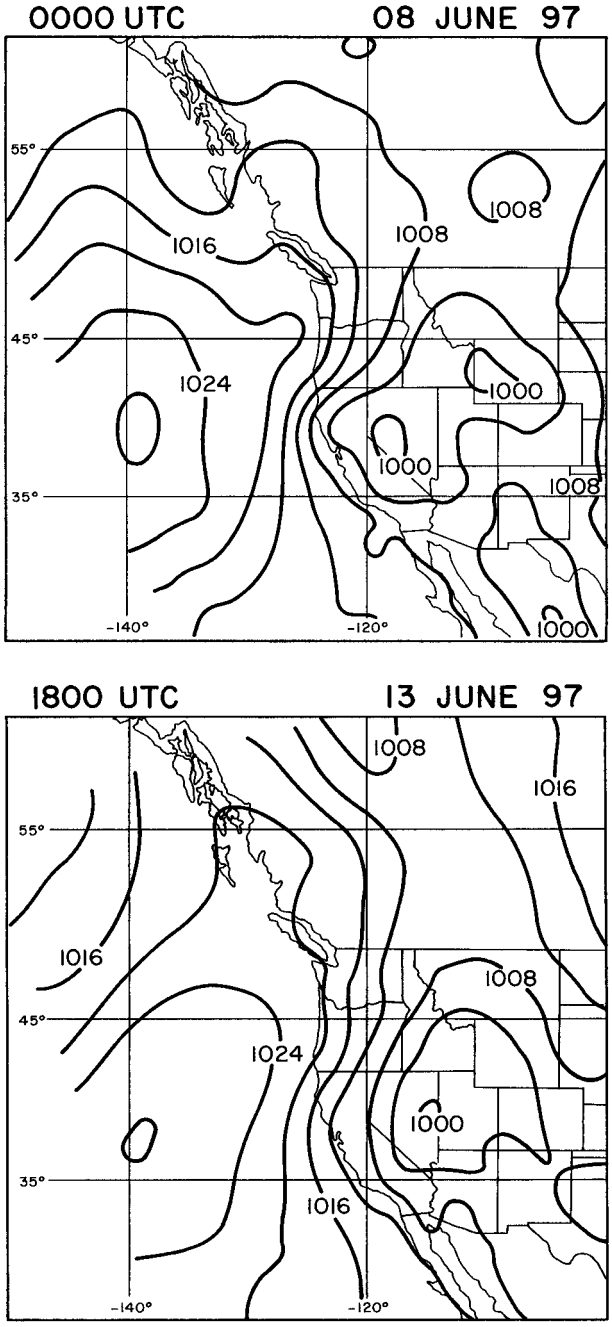

FIG. 1. Sea level pressure (hPa) at 0000 UTC 8 Jun and 1800 UTC 13 Jun 1997 taken from NCEP Eta Model analysis.

The depth of the inversion on 13 June can be seen to rise from less than 200 m at the easternmost sawtooth descent to approximately 500 m at the western end of the leg. The westward increase in the depth of the inversion is not as pronounced on 7 June. Potential temperatures increase by approximately 15° and 10°C across the inversion interface on 7 June and 13 June, respectively. Note that there is a general increase in the maximum wind speed as the MBL height increases. This reflects in part the smaller friction force experienced at the top of a deeper MBL. Profiles of dewpoint temperature (not shown) have the classic signature of a subsidence inversion with a moist boundary layer (relative humidity near 80%) capped by much drier air aloft (relative humidity near 20%). There is a suggestion that temperatures within the MBL increase to the west by 1.5°C or so over the length of the sawtooth on both days. This reflects the trend of sea surface temperatures with the coldest sea surface temperatures right at the coast. This is probably in response to coastal upwelling and is in agreement with previous observations (e.g., Zemba and Friehe 1987).

Cross sections of the total wind speed and potential temperature fields can be constructed from the east–west sawtooth flight legs along 37.5°N (Fig. 4). Wind speeds clearly follow the trends in the thermal field, and the isotach pattern slopes upward to the west. Note that the jet appears as a broad layer of strong wind rather than a local maximum for both case study days. The 13 June wind speed pattern in particular suggests a large horizontal extent of the CJ to the west of Half Moon Bay. A sloping MBL is clearly in evidence in Fig. 4 for both case study days. It is best exemplified on 13 June; a horizontal temperature gradient of approximately 7 K per 100 km is present on this day.

Cross sections of the total wind speed and potential temperature were constructed for the east–west sawtooth leg west of Monterey Bay along 36.8°N (Fig. 5) and the north–south sawtooth leg along 123.2°W on 7 June (Fig. 6). The cross-shore structure in Fig. 5 shows that the intensity of the CJ increases to the west of Monterey Bay similar to that observed to the north. Strongest winds are observed at least 100 km offshore here as well. The height of the maximum winds increases to the west similar to that observed in Fig. 4. The depth of the MBL increases by about 200 m over the approximately 75-km length of the sawtooth. Little variation in either wind speed or potential temperature was observed in the north–south direction along 123.2°W in Fig. 6.

Although the CJ has been previously documented, most observations of the CJ have been made within 25 km of the coast (Bridger et al. 1993). Only Bridger et al. (1993) and Rogers et al. (1998) describe the MBL at extended distances (in excess of 100 km) from the coast. Flights during June 1997 sampled the CJ at distances approaching 200 km from the coast. The June 1997 study has provided observational evidence as to the scale of the CJ, and observations collected during that period have prompted a slightly different explanation for the structure of the jet. There has been a considerable body of literature that focuses on the topographic interactions with the MBL (e.g., Dorman 1985; Beardsley et al. 1987; Samelson 1992). Hydraulic theory is used to explain the local accelerations of the wind about terrain irregularities such as points and capes. During the June 1997 flights, only weak and dif-

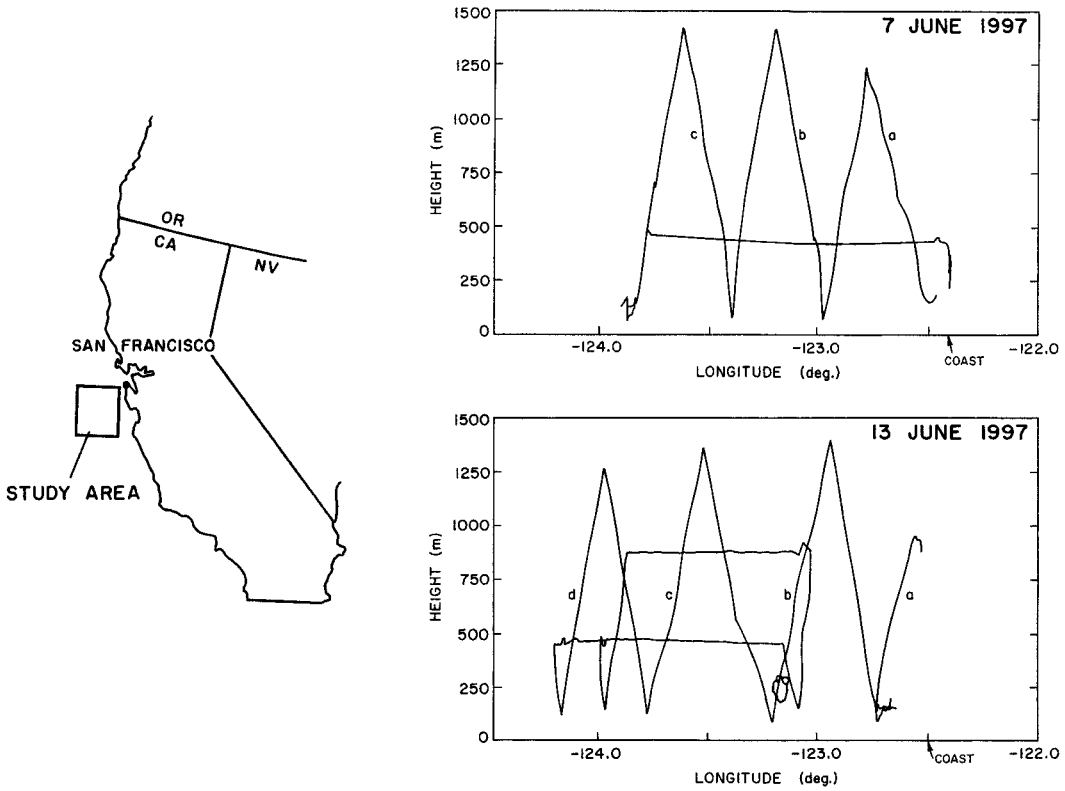

FIG. 2. Flight tracks for 7 and 13 Jun 1997 case study flights along 37.5°N.

fuse jetlike structures were seen near the coast. The environment within 10 km of the coast was tranquil on each of the seven flights. Little evidence of expansion fans or hydraulic jumps associated with the coastal terrain could be found. The CJ in each case, however, was well defined and characterized by its broad horizontal extent. This suggests that the CJ need not be associated with coastal topography and that the role of the local terrain in enhancing the CJ varies considerably from case to case.

The observed wind and potential temperature fields in Figs. 4 and 5 are consistent with the geostrophic adjustment of a thermally direct circulation arising due to the horizontal temperature contrast between the ocean and continent. The sloping marine inversion can be interpreted as a near-geostrophic frontal boundary between the cool maritime and the warmer continental air. The scale of the sloping MBL is consistent with that expected due to geostrophic adjustment. If one assumes an inversion strength of 8 K and an MBL height of 500 m, the Rossby radius of deformation is approximately 130 km. This is in good agreement with the observed scale of the MBL slope and attendant CJ during the June 1997 field study.

4. Forcing of the coastal jet

Horizontal pressure gradient forces drive atmospheric motions. To understand the forcing of the CJ, the PGF must be determined. From an observational point of view, accurate measurement of the PGF and hence the geostrophic wind is difficult. A 10 m s^{-1} geostrophic wind corresponds to an isobaric slope of only 10^{-4} in midlatitudes, or a change of 1 m over a distance of 10 km.

In situ measurements of the height of isobaric surfaces using instrumentation aboard research aircraft enables determination of the horizontal pressure gradient and, hence, the geostrophic wind. Airborne altimetry has been used by a number of investigators during the past two decades (e.g., Shapiro and Kennedy 1981, 1982; Brost et al. 1982; Zemba and Friehe 1987; Parish et al. 1988; Rodi and Parish 1988). Measurement of isobaric slopes using an airborne platform is conceptually simple. By flying at constant pressure, the height above ground of the isobaric surface can be determined by the onboard radar altimeter. The small deviations of the aircraft from the selected pressure level can easily be compensated for by a hydrostatic correction since temperatures are known to within 0.5°C. To find the horizontal pressure gradient, it is necessary to determine heights of an isobaric surface above some reference level, generally taken to be sea level. Over land this implies that both the terrain height of the underlying surface over which the plane passes and the geographic position (both longitude and latitude) of the aircraft must be known with a high degree of accuracy. By adding the

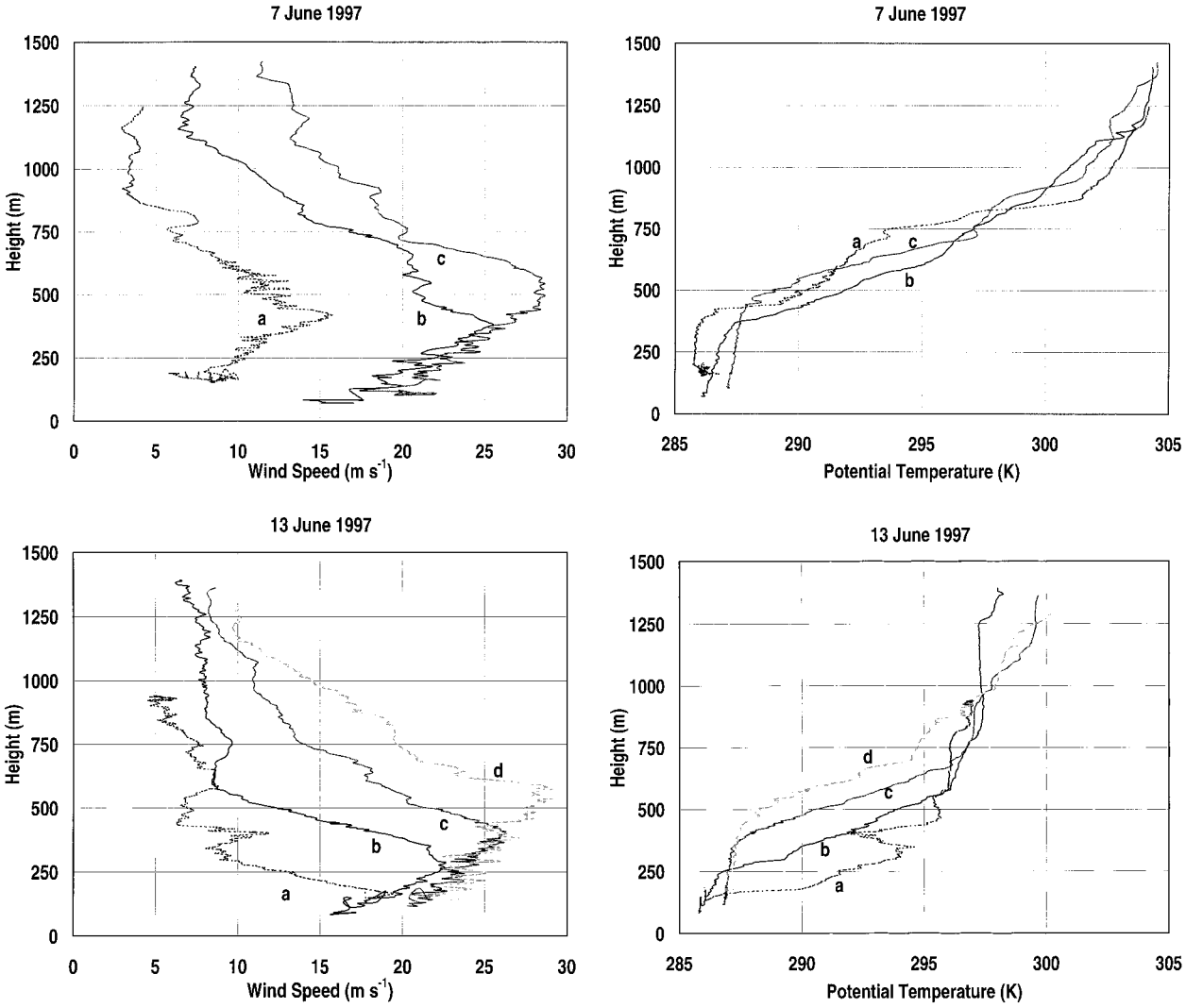

FIG. 3. Vertical profiles of wind speed (m s^{-1}) and potential temperature (K) obtained from east–west sawtooth flights along 37.5°N. Location of soundings is marked in Fig. 2.

radar altitude of the aircraft to the terrain height, an absolute measure of the height above sea level of the isobaric surface is obtained. The use of altimetry over the open ocean, as was done in this study, is even simpler since no terrain correction is required.

Several difficulties must be overcome to ensure accurate detection of the isobaric slopes. A summary of potential instrumentation errors can be found in Rodi and Parish (1988). An important consideration is the steady-state assumption implied in the time–space transformation during the calculation of the horizontal pressure gradient force. In a previous study of the Great Plains LLJ (Parish et al. 1988), the average leg length amounted to approximately 100 km and flight time averaged 20 min. Isallobaric tendencies were often large enough to mask the isobaric slope signal and thereby contaminate the geostrophic wind calculation, even during what appeared to be tranquil synoptic periods (geostrophic winds at flight level of less than 10 m s^{-1}). As an example, consider the case where geostrophic winds are from the north, such as in cases of the CJ, and pressures are falling uniformly. As the plane travels along a flight leg from west to east, the isobaric surface slopes downward. Because of the additional height fall of the isobaric surface during the duration of the flight leg, the plane appears to follow an exaggerated isobaric slope. On the return flight leg from east to west following the upward slope of the isobaric surface, the isallobaric tendency compensates for the natural geostrophic trend and the magnitude of the isobaric slope appears to be smaller than actually exists. The isobaric slope calculations thus show a directional bias. Even moderate pressure changes of 1 hPa h^{-1} correspond to isobaric height changes of approximately 8 m h^{-1}. This implies a 2.8-m height change during a 100-km flight leg of 20-min duration and an error in the geostrophic wind cal-

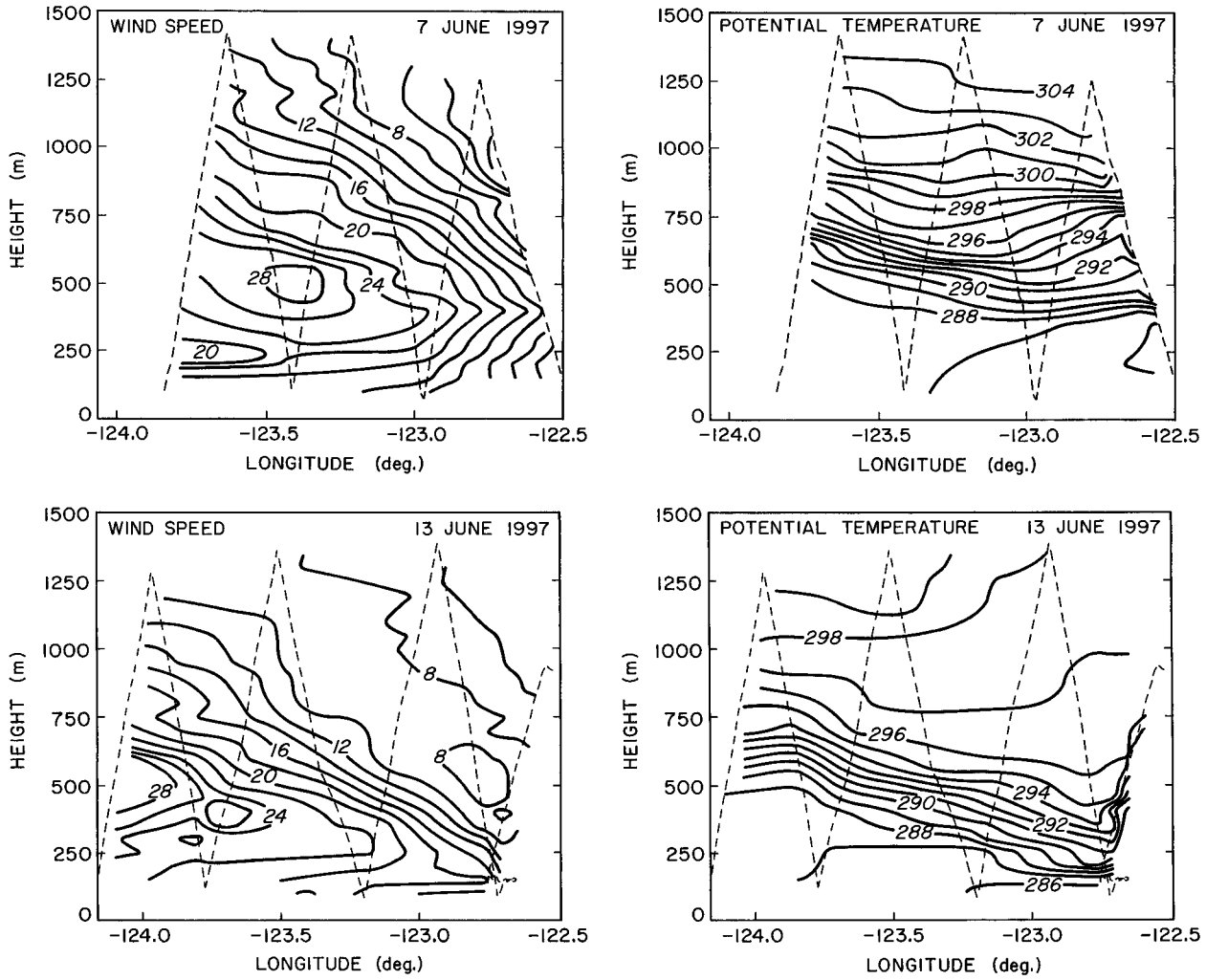

FIG. 4. Cross sections of wind speed (m s^{-1}) and potential temperature (K) from east–west sawtooth flight legs along 37.5°N on 7 and 13 Jun 1997. Dashed lines indicate aircraft track.

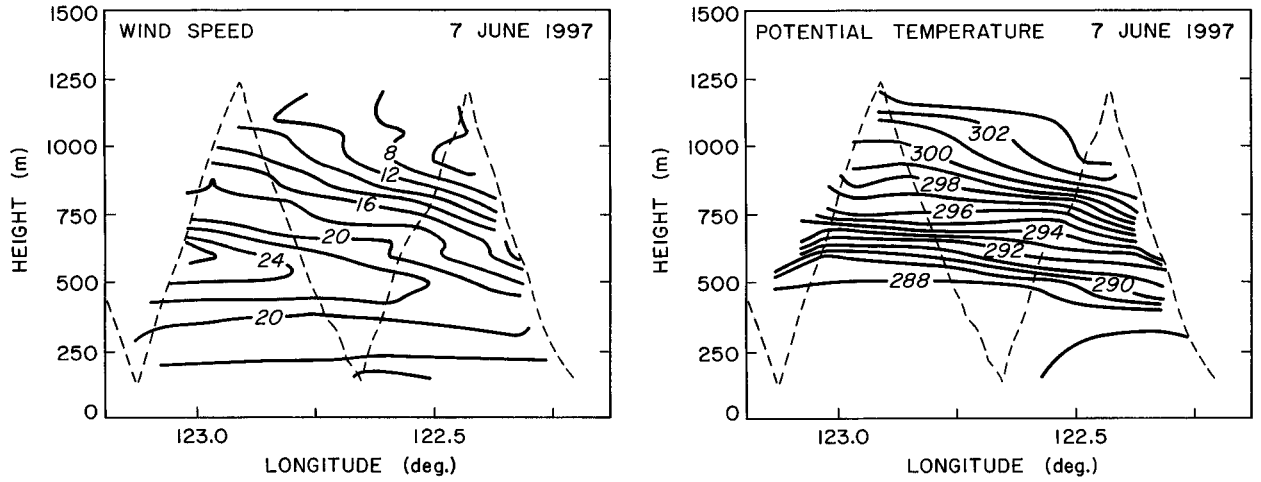

FIG. 5. Cross sections of wind speed (m s^{-1}) and potential temperature (K) from east to west leg along 36.8°N west of Monterey Bay on 7 Jun 1997. Dashed lines indicate aircraft track.

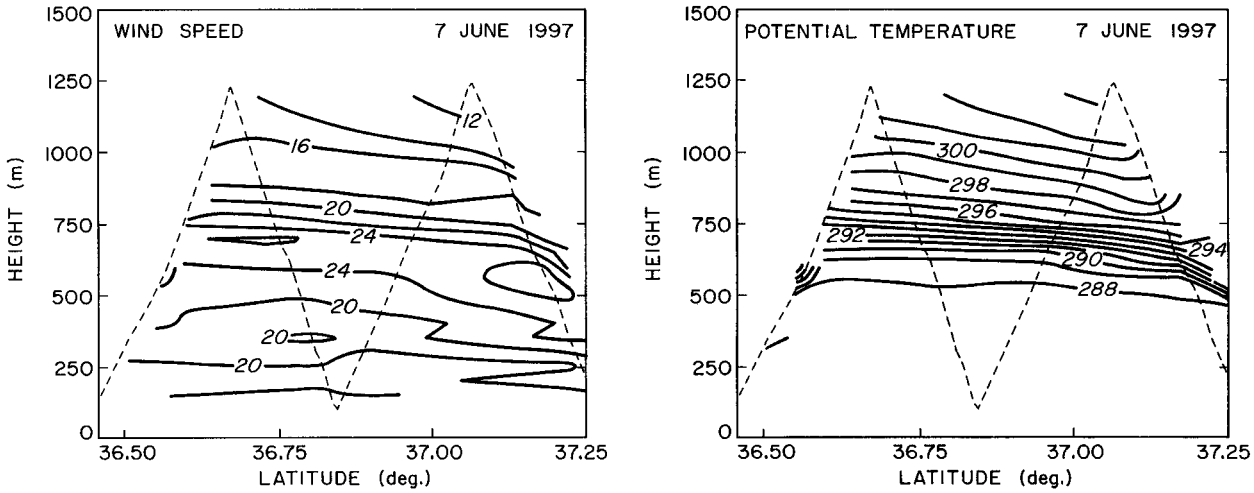

FIG. 6. As in Fig. 5, but for the north–south leg along 123.2°W on 7 Jun 1997.

culation of nearly 3 m s^{-1}. Redundant legs were shown to be necessary in the absence of detailed surface pressure information (Parish et al. 1988).

Redundant east–west legs at the 960-hPa level, near the level of the wind maximum, were conducted by the K/A for both the 7 and 13 June 1997 case studies along approximately 37.5°N (see Fig. 2). In addition, redundant north–south legs were also flown on 7 June along 123.2°W (time constraints only allowed one north–south leg on 13 June). The mean isobaric height changes amounted to a 0.4 m decrease in 20 min on 7 June and a 3.7 m decrease over a 35-min period on 13 June. An isallobaric correction was then made to eliminate this directional bias error in the PGF calculation. Corrected heights of the 960-hPa surface for the west–east flight legs are shown in Fig. 7a. The second east–west isobaric leg on 7 June is not shown in Fig. 7a since the trend is nearly identical to the first. Tracking of the isobaric surface was accomplished with high fidelity for all legs. Typical variations are on the order of 2 m. It should be noted that the underlying sea surface was often agitated in response to the strong northerly wind associated with the CJ. The actual ''noise'' in the isobaric height signal is no doubt influenced by water wave activity. Detection of the actual isobaric heights was much more precise than those attainable over land. Isobaric heights determined from previous work (e.g., Parish et al. 1988) can be seen to have far more uncertainty. It is thought that the deviations observed along the western half of the 13 June isobaric leg are real and possibly represent gravity wave activity along the inversion interface.

The mean PGF over each leg was computed by fitting a least-squares linear fit to the corrected isobaric heights in Fig. 7a. The mean slope of the isobaric surface corresponds to northerly geostrophic winds of 32.1 m s^{-1} on 7 June for the leg shown, and 21.4 and 25.4 m s^{-1} for the redundant legs on 13 June. Components of the wind along the isobaric legs are illustrated in Figs. 7b,c. The mean *y* component of the wind (Fig. 7c) was 27.2 m s^{-1} for the 7 June case shown, and 20.6 and 21.3 m s^{-1} for the two legs on 13 June. The motion is thus close to geostrophic balance. It is not known what physical mechanisms are responsible for the subgeostrophic nature of the flow, although friction is a logical possibility. The track of the K/A along the 960-hPa surface commenced at the west end near the level of the jet core. As the aircraft moves east, the elevation of the MBL and hence level of the jet core decreases. The slope of the inversion surface is thus considerably greater than the slope of an isobaric surface and the K/A track does not fly at the level of strongest winds throughout the course of the entire leg.

The variation of the *y* component of the wind shows that the isobaric flight leg intercepted the top of the MBL near 123.2°W on 7 June and 123.7°W on 13 June. Isobaric wind speeds decrease toward the east as the K/A moves through the top of the MBL. Pronounced differences in the variance of the wind speed are also evident from Fig. 7c and match expectations regarding the turbulent nature of the MBL. The *x* components (Fig. 7b) average 8.5 m s^{-1} over the isobaric leg and mirror the trends in wind speed and turbulent intensity displayed by the *y* components.

A 910-hPa isobaric leg was also conducted on 13 June, sandwiched between the 960-hPa legs. This leg was directed from east-to-west at approximately the 900-m level, which is above the MBL. Measurement of the horizontal pressure gradient over the entire leg length (Fig. 8a) revealed a mean northerly geostrophic wind of 9.6 m s^{-1}. Wind speeds in Fig. 8b reflect trends seen in the boundary layer and are proportional to the relative height above the MBL. The K/A track commenced on the east side at a level approximately 700 m above the top of the MBL and reached the westernmost point approximately 250 m above the of the MBL. The strongest winds were observed at the western end

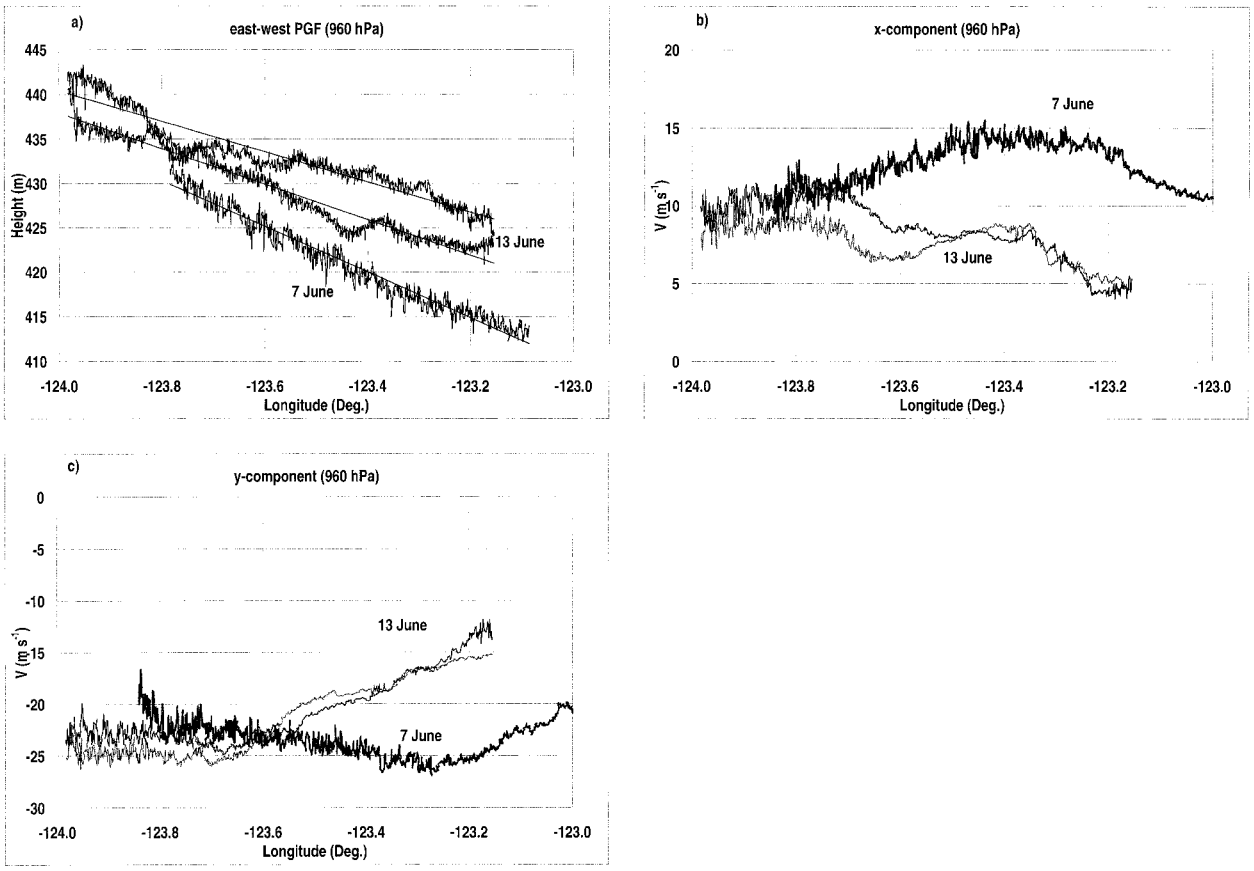

FIG. 7. The K/A measurements of (a) corrected isobaric heights of 960-hPa surface (m), (b) *x* component of wind for east–west legs (m s^{-1}) on 7 and 13 Jun 1997, and (c) *y* component of wind (m s^{-1}). Straight line on isobaric heights represents least squares linear fit, the slope of which determines the geostrophic wind.

of the leg with speeds of approximately 15 m s^{-1}. The mean *y* component of the wind speed for the entire leg was 10.0 m s^{-1} indicating that the flow above the inversion was nearly geostrophic as well. The *x* component of the wind field was near zero throughout this leg.

Coastal LLJs are predominately oriented in a direction parallel to the coastline. The California coastline near Half Moon Bay has a general trend from NNW to SSE. Flights were also conducted in the north–south direction within the MBL to examine the dynamics of the forcing of the *x* component of the geostrophic wind. Figure 9a illustrates the isobaric height traces for both cases. The 7 June north–south leg was conducted at 960-hPa, corresponding to a height of approximately 400 m above the ocean. The 13 June flight leg was at the 980-hPa level or 260 m above the ocean. Both north–south legs remain within the MBL for entire leg. The trend of the isobaric heights from north to south is upward, consistent with a westerly component of the geostrophic wind. The least squares linear fit indicates a geostrophic wind in the *x* direction of 18.0 and 14.2 m s^{-1} on 7 and 13 June, respectively, compared to the mean *x* component of the wind speed of 12.9 and 12.1 m s^{-1}.

The resulting ageostrophic winds on 7 June of approximately 5 m s^{-1} are reasonable from the observed *y* components of the wind. Figure 9c shows that the *y* components of the flow undergo a deceleration from approximately 23 m s^{-1} to 19 m s^{-1} over a 100-km distance. Following Holton (1992, p. 175), the change in the wind speeds along a streamline can be related to an ageostrophic component of motion. A 9-m s^{-1} ageostrophic component directed west results from changes in the *y* components of the wind speed observed on 7 June. As seen for the east–west legs, there may be some frictional slowing of the wind as well that can account for some of the ageostrophic nature of the flow. A second north–south leg was conducted at approximately 940 Pa on 13 June to measure the forcing above the MBL. Results (not shown) reveal an equivalent geostrophic wind of 3.3 m s^{-1}. The mean *x* component of the wind for this leg was again from the west at 2.5 m s^{-1}, suggesting that winds here are reasonably close to geostrophic as well.

Given that the two horizontal components of the geostrophic wind are within or near the MBL, it is possible to infer the total geostrophic wind vector for both days. Assuming that the geostrophic wind is roughly uniform in the vertical below the inversion, the *x* and *y* com-

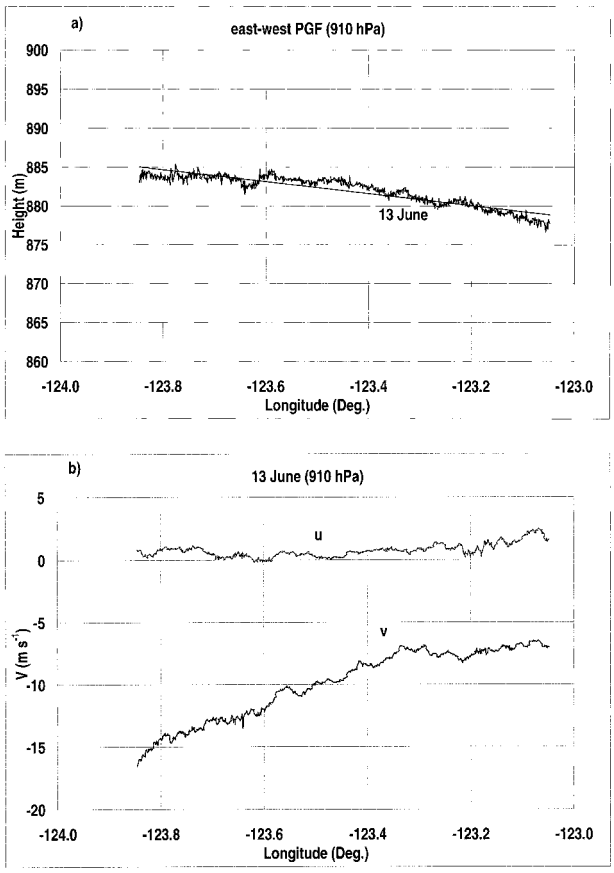

FIG. 8. The K/A measurements of (a) corrected isobaric heights (m) and (b) *x* and *y* wind components (m s^{-1}) on 13 Jun 1997 along the 910-hPa surface.

ponents of the geostrophic wind are approximately 18 and 32 m s^{-1}, respectively, on 7 June and 14 m s^{-1} and 23 m s^{-1}, respectively, on 13 June. Thus, the magnitude of the geostrophic wind is 36 m s^{-1} on 7 June and 27 m s^{-1} on 13 June. In both cases the geostrophic wind direction is approximately 330°. This PGF is perpendicular to the coastline and hence the geostrophic wind is directed parallel to the coastline. Given the importance of the spatial pattern of diabatic heating on the establishment of the PGF, this result is to be expected.

One intriguing result of these flights is the nonuniform nature of the isobaric heights. The PGFs observed during the June 1997 experiment were obtained under ideal conditions. Analyses of isobaric heights collected during redundant flight legs often revealed wave activity and other nonsteady behavior of isobaric legs (Fig. 7a). Results from these and other case studies of the CJ during June 1997 clearly illustrate the transient nature of the PGF over mesoscale distances. Parish et al. (1988) proposed that detection of isobaric slopes with an effective accuracy of 0.5 m s^{-1} is possible using radar altimetry. Results from the California field study have forced a reexamination of this estimate. Note the differences in the height of the isobaric surface for the 13 June legs. Not only does the mean height of the 960-hPa surface change, but also some significant local variations are present. This is testimony to the small-scale variation that is present in the atmosphere. Observed trends in the isobaric heights illustrate the complex and transitory nature of the horizontal pressure gradient force. Originally it was expected that determination of the PGF over the water surface would be possible to within an equivalent geostrophic wind of 1 m s^{-1}. It is now thought that the fundamental limitation to the accuracy of PGF measurements by airborne altimetry is not due to measurement sensitivity, but rather because of the inherent variability in the small-scale atmospheric forcing. Geostrophic winds are thus only meaningful to approximately 3 m s^{-1} over distances of 50 km.

5. Thermal wind calculations

Additional estimates of the isobaric slopes can be obtained from the sawtooth legs. For example, Fig. 2 shows that a total of four descents and three ascents were conducted as part of the sawtooth leg on 13 June. Data for this case were then sorted by pressure and divided into 10-hPa classes. Each observation was then reduced to a common isobaric level for each class using a hydrostatic correction. This provided clusters of points at seven locations along the 13 June sawtooth leg to define the isobaric slopes. The geostrophic wind calculations using this method are not as accurate as those determined from isobaric flight legs since the total number of data points available is less than that obtained during the isobaric flight legs, but there is no reason to question the results. In addition, thermal wind estimates can be obtained by examination of temperature gradients at the various levels to serve as a check on the shear of the inferred geostrophic wind at the various levels.

Figure 10 summarizes the calculations for the *y*-component of the geostrophic wind over the 13 June sawtooth leg. It is important to point out that this leg is approximately 150 km in length, nearly twice as long as the isobaric legs discussed earlier. As can be inferred form Fig. 2, the PGF measured as part of the sawtooth maneuvers encompasses a region nearly 80 km to the east of the isobaric legs. Hence the calculated geostrophic winds may differ slightly from those determined from the isobaric legs. Since the maximum CJ winds decrease to the east, it was expected that the calculated magnitude of the geostrophic winds along the sawtooth would be less than those obtained from the 13 June isobaric legs. The maximum *y* component of the geostrophic wind speed along the sawtooth maneuver was 22 m s^{-1} at 250 m, decreasing with height to approximately 12 m s^{-1} at the level of the inversion. Comparison with actual *y* components shows significantly subgeostrophic winds in the lowest 400 m, presumably due to frictional influence. Winds, however, were close to geostrophic near the top of the MBL. Since isobaric temperature gradients along the *x* direction could be

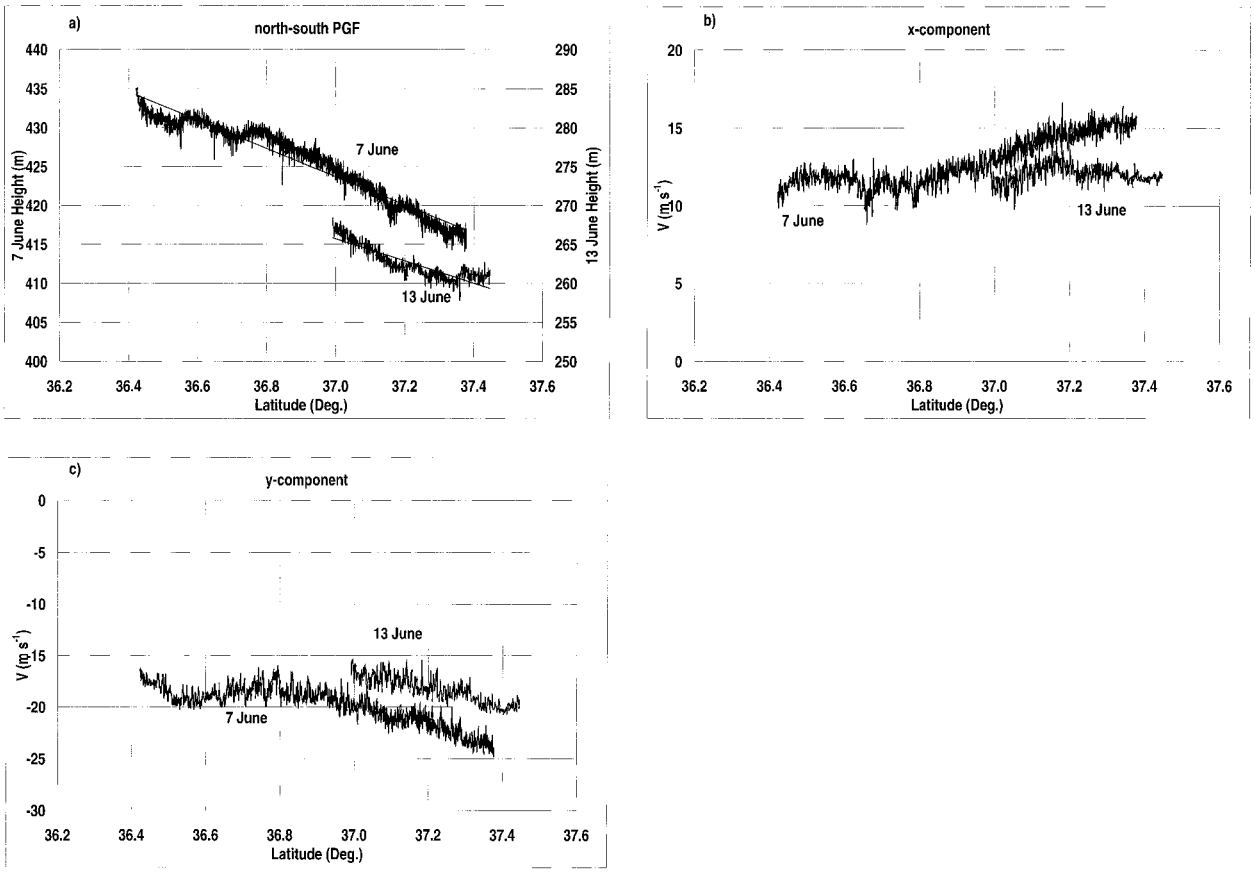

FIG. 9. The K/A measurements of (a) corrected isobaric heights (m), (b) *x* component of wind (m s^{-1}), and (c) *y* component of wind (m s^{-1}) for north–south legs on 7 and 13 Jun 1997.

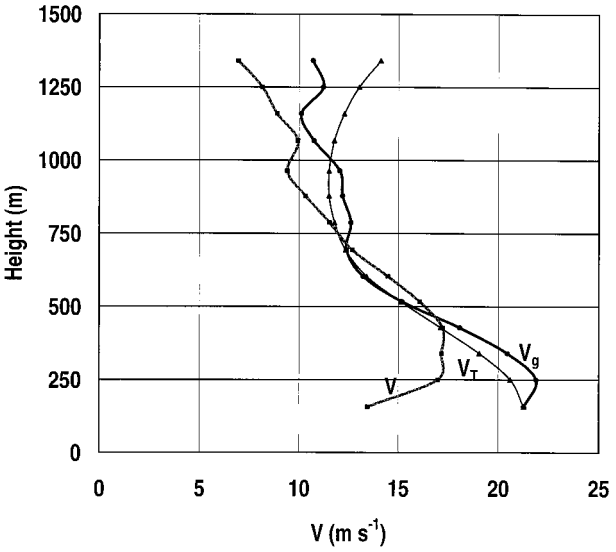

FIG. 10. Profiles of *y* component of wind (V), *y* component of the geostrophic wind (V_g), and calculated geostrophic wind profile (V_T) obtained by adding thermal wind components to lowest-level geostrophic wind component for 13 Jun 1997 case study.

inferred, the *y* component of the thermal wind could be calculated. The thermal wind is simply a measure of the vertical shear of the geostrophic wind. An alternate mean of computing the geostrophic wind profile in the *y* direction can then be estimated by summing up the thermal wind components, assuming that the geostrophic wind is known at one level. Here it is assumed that the geostrophic wind at the lowest level (980 hPa, approximately 250 m) is used to start the thermal wind computation.

Figure 10 illustrates the estimated *y*-component of the geostrophic wind profile, obtained by integrating the thermal wind equation from the 980-hPa level. It can be seen that the measured geostrophic wind profile is in reasonable agreement with the measured geostrophic wind profile from the sawtooth legs. It can be concluded that the CJ observed on 13 June 1997 represents a situation that is close to geostrophic and thermal wind balance over a scale of motion at least 150 km in horizontal extent.

6. Summary

Airborne missions were undertaken on 7 and 13 June 1997 to study the kinematics and dynamics of the CJ

off the coast of California. The emphasis was to provide observational evidence as to the forcing of the CJ. A flight strategy was designed to allow a large volume of the lower troposphere to be sampled in the cross-shore direction to enable visualization of the horizontal and vertical structure of wind and temperatures associated with the CJ.

Results from the case studies suggest that the CJ extends over a horizontal scale on the order of the Rossby radius of deformation. Winds are near-geostrophic at the top of the MBL. A sloping MBL and attendant thermal field offshore from the coastline was present for all case study days. The depth of the boundary layer along the 37.5°N latitude flight track on 13 June increases from less than 200 m near the coast to greater than 500 m at the west end some 150 km away. It is offered that the westward increase in the MBL depth is the result of geostrophic adjustment in the cross-coast direction due to the pronounced thermal gradients at the coast. The differential heating between ocean and land forces a thermally direct circulation that results in a sloping frontal structure of the MBL, separating the cool maritime air from the warm continental air. Horizontal temperature gradients and hence a thermal wind result from this adjustment process and are responsible for the rapid decrease in wind speed about the inversion as previously noted. The data collected during June 1997 suggest that local hydraulic effects need not be operating for a well-developed CJ to exist.

It can be concluded that the forcing of the CJ near the California coast differs in structure and origin from other examples of the LLJ. In particular, the geostrophic nature of this LLJ class of flows contrasts significantly with the often-discussed Great Plains LLJ that occurs as a result of inertial oscillations of significant ageostrophic components.

Acknowledgments. The author wishes to thank participants in the field study, including Glenn Gordon, Larry Oolman, Dave Leon, Sam Haimov, Liz Sinclair, Mark Hoshor, Ernest Gasaway, Larry Irving, Jim Waldram, and Susan Fitzgerald. Special thanks go out to Wendell Nuss, who provided accurate forecasts throughout the period, and John Bane for his discussions pertaining to the marine boundary layer. This research was funded by the Office of Naval Research through Grant N00014-96-1-1236.

REFERENCES

Arritt, R. W., T. D. Rink, M. Segal, D. P. Todey, C. A. Clark, M. J. Mitchell, and K. M. Labas, 1997: The Great Plains low-level jet during the warm season of 1993. *Mon. Wea. Rev.,* **125,** 2176–2192.

Beardsley, R. C., C. E. Dorman, C. A. Friehe, L. K. Rosenfield, and C. D. Wyant, 1987: Local atmospheric forcing during the Coastal Ocean Dynamics Experiment 1: A description of the marine boundary layer and atmospheric conditions over a northern California upwelling region. *J. Geophys. Res.,* **92,** 1467–1488.

Bell, G. D., and L. F. Bosart, 1988: Appalachian cold-air damming. *Mon. Wea. Rev.,* **116,** 137–161.

Blackadar, A. K., 1957: Boundary layer wind maxima and their significance for the growth of nocturnal inversion. *Bull. Amer. Meteor. Soc.,* **38,** 283–290.

Bond, N. A., C. F. Mass, and J. E. Overland, 1996: Coastally trapped wind reversals along the United States West Coast during the warm season. Part 1: Climatology and temporal evolution. *Mon. Wea. Rev.,* **124,** 430–445.

Bonner, W. D., 1968: Climatology of the low-level jet. *Mon. Wea. Rev.,* **96,** 833–850.

Bridger, A. F. C., W. C. Brick, and P. F. Lester, 1993: The structure of the marine inversion layer off the central California coast: Mesoscale conditions. *Mon. Wea. Rev.,* **121,** 335–351.

Brill, K. F., L. W. Uccellini, R. P. Burkhart, T. T. Warner, and R. A. Anthes, 1985: Numerical simulations of a transverse indirect circulation and low level jet in the exit region of an upper-level jet. *J. Atmos. Sci.,* **42,** 1306–1320.

Brost, R. A., D. H. Lenschow, and J. C. Wyngaard, 1982: Marine stratocumulus layers: Mean conditions. *J. Atmos. Sci.,* **39,** 800–817.

Burk, S. D., and W. T. Thompson, 1996: The summertime low-level jet and marine boundary layer structure along the California coast. *Mon. Wea. Rev.,* **124,** 668–686.

——, T. Haack, and R. M. Samuelson, 1999: Mesoscale simulations of supercritical, subcritical, and transcritical flow along coastal topography. *J. Atmos. Sci.,* **56,** 2780–2795.

Chao, S.-Y., 1985: Coastal jets in the lower atmosphere. *J. Phys. Oceanogr.,* **15,** 361–371.

Dorman, C. E., 1985: Evidence of Kelvin waves in California's marine layer and related eddy generation. *Mon. Wea. Rev.,* **113,** 827–839.

Douglas, M. W., 1995: The summertime low-level jet over the Gulf of California. *Mon. Wea. Rev.,* **123,** 2334–2347.

Doyle, J. D., and T. T. Warner, 1991: A Carolina coastal low-level jet during GALE IOP 2. *Mon. Wea. Rev.,* **119,** 2414–2428.

Elliot, D. L., and J. J. O'Brien, 1977: Observational studies of the marine boundary layer over an upwelling region. *Mon. Wea. Rev.,* **105,** 86–98.

Gerber, H., S. Chang, and T. Holt, 1989: Evolution of a marine boundary layer jet. *J. Atmos. Sci.,* **46,** 1312–1326.

Hoecker, W. H., 1963: Three southerly low-level jet systems delineated by the Weather Bureau special pibal network in 1961. *Mon. Wea. Rev.,* **91,** 573–582.

Holt, T. R., 1996: Mesoscale forcing of a boundary layer jet along the California coast. *J. Geophys. Res.,* **101,** 4235–4254.

Holton, J. R., 1967: The diurnal boundary layer wind oscillation above sloping terrain. *Tellus,* **19,** 199–205.

——, 1992: *An Introduction to Dynamic Meteorology.* Academic Press, 511 pp.

Kaimal, J. C., and Y. Izumi, 1965: Vertical velocity fluctuations in a nocturnal low-level jet. *J. Appl. Meteor.,* **4,** 576–584.

Lester, P. F., 1985: Studies of the marine inversion over the San Francisco Bay area. A summary of the work of Albert Miller, 1961–1978. *Bull. Amer. Meteor. Soc.,* **66,** 1396–1402.

Li, J., and Y.-L. Chen, 1998: Barrier jets during TAMEX. *Mon. Wea. Rev.,* **126,** 959–971.

McNider, R. T., and R. A. Pielke, 1981: Diurnal boundary-layer development over sloping terrain. *J. Atmos. Sci.,* **38,** 2198–2212.

Neiburger, M., D. S. Johnson, and C. W. Chien, 1961: Studies of the structure of the atmosphere over the eastern Pacific Ocean in the summer. *The Inversion Over the Eastern North Pacific Ocean,* University of California Press, 1–94.

Nuss, W., 1995: Lee troughing and the evolution of a coastally-trapped disturbance. Preprints, *Seventh Conf. on Mountain Meteorology,* Breckenridge, CO, Amer. Meteor. Soc., 212–215.

Parish, T. R., 1982: Barrier winds along the Sierra Nevada Mountains. *J. Appl. Meteor.,* **21,** 925–930.

——, 1983: The influence of the Antarctic Peninsula on the windfield over the western Weddell Sea. *J. Geophys. Res.,* **88,** 2684–2692.

——, A. R. Rodi, and R. D. Clark, 1988: A case study of the summertime Great Plains low-level jet. *Mon. Wea. Rev.*, **116,** 94–105.

Ralph, F. M., J. M. Bane, C. Dorman, W. D. Neff, P. J. Neiman, W. Nuss, and P. O. G. Persson, 1998: Observations and analysis of the 10–11 June 1994 coastally trapped disturbance. *Mon. Wea. Rev.*, **126,** 2435–2465.

Rodi, A. R., and T. R. Parish, 1988: Aircraft measurement of mesoscale pressure gradients and ageostrophic winds. *J. Atmos. Oceanic Technol.*, **5,** 91–101.

Rogers, D. P., and Coauthors, 1998: Highlights of Coastal Waves 1996. *Bull. Amer. Meteor. Soc.*, **79,** 1307–1326.

Samelson, R. M., 1992: Supercritical marine-layer flow along a smoothly varying coastline. *J. Atmos. Sci.*, **49,** 1571–1584.

——, and S. J. Lentz, 1994: The horizontal momentum balance in the marine atmospheric boundary layer during CODE-2. *J. Atmos. Sci.*, **51,** 3745–3757.

Schwerdtfeger, W., 1979: Meteorological aspects of the drift of ice from the Weddell Sea toward the middle-latitude westerlies. *J. Geophys. Res.*, **84,** 6321–6327.

Shapiro, M. A., and P. J. Kennedy, 1981: Research aircraft measurements of jet stream geostrophic and ageostrophic winds. *J. Atmos. Sci.*, **38,** 2642–2652.

——, and ——, 1982: Airborne radar altimeter measurements of geostrophic and ageostrophic winds over irregular terrain. *J. Appl. Meteor.*, **21,** 1739–1746.

Uccellini, L. W., and D. R. Johnson, 1979: The coupling of upper and lower tropospheric jet streams and implications for the development of severe convective storms. *Mon. Wea. Rev.*, **107,** 682–703.

Whiteman, C. D., X. Bian, and S. Zhong, 1997: Low-level jet climatology from enhanced rawinsonde observations at a site in the southern Great Plains. *J. Appl. Meteor.*, **36,** 1363–1376.

Winant, C. D., C. E. Dorman, C. A. Friehe, and R. C. Beardsley, 1988: The marine layer off northern California: An example of supercritical channel flow. *J. Atmos. Sci.*, **45,** 3588–3605.

Zemba, J., and C. A. Friehe, 1987: The marine boundary layer jet in the coastal ocean dynamics experiment. *J. Geophys. Res.*, **92,** 1489–1496.